encit 2020

ABCM Associação Brasileira de Engenharia e Ciências Mecânicas

18th Brazilian Congress of Thermal Sciences and Engineering
November 16-20, 2020 (Online)

ENC-2020-694
NATURAL CONVECTION IN A HORIZONTAL ANNULUS FILLED WITH POROUS MEDIA WITH INTERNAL HEAT GENERATION

Beatriz Machado dos Santos
Jian Su
Universidade Federal do Rio de Janeiro
bmachado@coppe.ufrj.br
sujian@nuclear.ufrj.br

Abstract. *The generalized integral transform technique (GITT), a hybrid numerical-analytical method, is proposed to investigate the steady-state natural convection in an annulus porous cavity with volumetric heat generation. The resulting system of non-linear ordinary differential equations, for temperature and stream function, through performing the GITT is numerically solved by the finite difference method. Purely numerical solutions, using the finite difference method, were performed to validate the results obtained previously. The calculations were performed in the computational software Mathematica.*

Keywords: *natural convection, generalized integral transform technique, horizontal annulus*

1. INTRODUCTION

Natural convection in cavities is a topic of great interest to researchers in the heat and mass transfer field, given its importance in industry and other engineering applications, such as, dry storage of nuclear spent fuel. Numerical, analytical and experimental investigations about natural convection phenomena were performed in the last decades, especially in cavities with internal heat generation with different geometries, among them, rectangular cavities (Lee and Goldstein, 1988; Joshi *et al.*, 2006), vertical cylinders (Martin, 1967; Holzbecher and Steiff, 1995) and horizontal annulus (Shekar *et al.*, 1984; Yuan *et al.*, 2015).

Vasseur *et al.* (1984) performed a numerically investigation of the natural convection in an annular porous layer with internal heat generation. The finite-difference method was used to solve the 2-D Darcy-Oberbeck-Boussinesq equations.

Baohua and Cotta (1993) proposed the generalized integral transform technique (GITT), which is a hybrid numerical-analitical approach, to study steady state natural convection in a saturated porous vertical rectangular enclosure subjected to uniform internal heat generation. The solutions were obtained in the stream function-temperature formulation and the results were compared with purely numerical solutions previously reported on the literature.

In this work, GITT is applied to solve the governing equations in stream-function, combining integral transform and finite difference method. Excellent convergence is shown for both stream-function and temperature.

2. GOVERNING EQUATIONS

The problem considered is a two-dimensional, steady natural convection in a saturated porous annulus enclosure with internal heat generation. The porous medium is isotropic, homogeneous and saturated with an incompressible fluid. The internal and external walls are kept at constant and uniform temperature and the heat is generated by a uniformly distributed energy source within the cavity. The top and bottom ends are kept insulated, as shown in Fig. 1.

After considering the Boussinesq approximation and the validity of Darcy's law, the dimensionless form of the problem formulation is represented by Eq. (1).

$$\frac{\partial^2\psi(r,\theta)}{\partial r^2}+\frac{1}{r}\frac{\partial\psi(r,\theta)}{\partial r}+\frac{1}{r^2}\frac{\partial^2\psi(r,\theta)}{\partial\theta^2}=-Ra\left(\frac{\partial T(r,\theta)}{\partial r}\sin\theta+\frac{\cos\theta}{r}\frac{\partial T(r,\theta)}{\partial\theta}\right),\ in\ r_0<r<1,\ 0<\theta<\pi \quad (1a)$$

$$\frac{\partial^2T(r,\theta)}{\partial r^2}+\frac{1}{r}\frac{\partial T(r,\theta)}{\partial r}+\frac{1}{r^2}\frac{\partial^2T(r,\theta)}{\partial\theta^2}+1=\frac{1}{r}\frac{\partial\psi(r,\theta)}{\partial\theta}\frac{\partial T(r,\theta)}{\partial r}-\frac{1}{r}\frac{\partial\psi(r,\theta)}{\partial r}\frac{\partial T(r,\theta)}{\partial\theta},\ in\ r_0<r<1,\ 0<\theta<\pi \quad (1b)$$

with the following boundary conditions

$$\psi(r_0,\theta)=\psi(1,\theta)=0,\quad T(r_0,\theta)=T(1,\theta)=0 \qquad (1c-f)$$

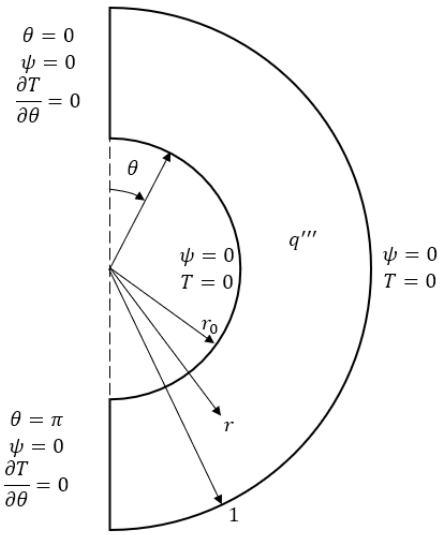

Figure 1: Coordinate system and flow geometry.

$$\psi(r,0) = \psi(r,\pi) = 0, \quad \frac{\partial T(r,0)}{\partial \theta} = \frac{\partial T(r,\pi)}{\partial \theta} = 0 \tag{1g-j}$$

where the Eqs. (1c-f) corresponds to the case of internal and external walls impermeable and kept at the same and constant temperature and Eqs. (1g-j) represents the symmetry across the vertical axis.

The dimensionless Darcy velocities (u and v) in cylindrical coordinates in terms of the stream function are presented in the Eqs. (2a,b).

$$u = \frac{1}{r}\frac{\partial \psi(r,\theta)}{\partial \theta}, \quad v = -\frac{\partial \psi(r,\theta)}{\partial r} \tag{2a,b}$$

In order to solve the problem by the generalized integral transform technique, the appropriate auxiliary problems must be chosen. Equations (3) and (4) show the auxiliary problems used.

$$\frac{\mathrm{d}^2\chi_i(\theta)}{\mathrm{d}\theta^2} + \mu_i^2\chi_i(\theta) = 0, \;\; 0 < \theta < \pi, \tag{3a}$$

$$\chi_i(0) = 0, \;\; \chi_i(\pi) = 0, \;\; i = 1,2,3,.. \tag{3b}$$

and

$$\frac{\mathrm{d}^2\Gamma_n(\theta)}{\mathrm{d}\theta^2} + \lambda_n^2\Gamma_n(\theta) = 0, \;\; 0 < \theta < \pi, \tag{4a}$$

$$\frac{\mathrm{d}\Gamma_n(0)}{\mathrm{d}\theta} = 0, \;\; \frac{\mathrm{d}\Gamma_n(\pi)}{\mathrm{d}\theta} = 0, \;\; n = 1,2,3,... \tag{4b}$$

where the eigenfunctions are presented by Eq. (5) and (6), and the eigenvalues are μ_i and λ_n.

$$\chi_i(\theta) = \sqrt{\frac{2}{\pi}}\sin(\mu_i\theta), \;\; \mu_i = i, \;\; i = 1,2,3,... \tag{5}$$

$$\Gamma_n(\theta) = \sqrt{\frac{2}{\pi}}\cos(\lambda_n\theta)^1, \;\; \lambda_n = n, \;\; n = 1,2,3,... \tag{6}$$

The integral transform pair is defined by Eq. (7) to the streamfunction and Eq. (8) to the temperature. The first equation in the braces is the transform and the second is the inversion formulae.

$$\begin{cases} \overline{\psi_i}(r) = \displaystyle\int_0^\pi \chi_i(\theta)\psi(r,\theta)\mathrm{d}\theta, \;\; transform, \\ \psi(r,\theta) = \displaystyle\sum_{i=1}^{\infty} \chi_i(\theta)\overline{\psi_i}(r), \;\; inversion, \end{cases} \tag{7}$$

$$\begin{cases} \overline{T_n}(r) = \displaystyle\int_0^\pi \Gamma_n(\theta)T(r,\theta)\mathrm{d}\theta, \;\; transform, \\ T(r,\theta) = \displaystyle\sum_{i=1}^{\infty} \Gamma_n(\theta)\overline{T_n}(r), \;\; inversion. \end{cases} \tag{8}$$

Operating Eq. (1a) with $\int_0^\pi \chi_i(\theta)\mathrm{d}\theta$

$$\frac{\partial^2\overline{\psi_i}(r)}{\partial r^2} + \frac{1}{r}\frac{\partial\overline{\psi_i}(r)}{\partial r} - \frac{\mu_i^2}{r^2}\overline{\psi_i}(r) = -Ra\left(\int_0^\pi \chi_i(\theta)\frac{\partial T(r,\theta)}{\partial r}\sin\theta\mathrm{d}\theta + \int_0^\pi \chi_i(\theta)\frac{\cos\theta}{r}\frac{\partial T(r,\theta)}{\partial\theta}\mathrm{d}\theta\right) \tag{9a}$$

Operating Eq. (1b) with $\int_0^\pi \Gamma_n(\theta)\mathrm{d}\theta$

$$\frac{\partial^2\overline{T_n}(r)}{\partial r^2} + \frac{1}{r}\frac{\partial\overline{T_n}(r)}{\partial r} - \frac{\lambda_n^2}{r^2}\overline{T_n}(r) + \overline{f_n} = \int_0^\pi \Gamma_n(\theta)\frac{1}{r}\frac{\partial\psi(r,\theta)}{\partial\theta}\frac{\partial T(r,\theta)}{\partial r}\mathrm{d}\theta - \int_0^\pi \Gamma_n(\theta)\frac{1}{r}\frac{\partial\psi(r,\theta)}{\partial r}\frac{\partial T(r,\theta)}{\partial\theta}\mathrm{d}\theta \tag{9b}$$

where the transformed heat generation term becomes

$$\overline{f_n} = \int_0^\pi \Gamma_n(\theta)\mathrm{d}\theta \equiv \sqrt{\pi} \tag{9c}$$

The non-transformable terms are presented by Eqs. (10).

$$\int_0^\pi \chi_i(\theta)\frac{\partial T(r,\theta)}{\partial r}\sin\theta\mathrm{d}\theta = \sum_{j=1}^{\infty} a_{ij}\frac{\partial\overline{T_j}(r)}{\partial r} \tag{10a}$$

$$a_{ij} = \int_0^\pi \chi_i(\theta)\sin(\theta)\Gamma_j(\theta)\mathrm{d}\theta \tag{10b}$$

$$\int_0^\pi \chi_i(\theta)\frac{\cos\theta}{r}\frac{\partial T(r,\theta)}{\partial\theta}\mathrm{d}\theta = \frac{1}{r}\sum_{j=1}^{\infty} a_{ij}^*\overline{T_j}(r) \tag{10c}$$

$$a_{ij}^* = \int_0^\pi \chi_i(\theta)\cos(\theta)\Gamma_j^{'}(\theta)\mathrm{d}\theta \tag{10d}$$

$$\int_0^\pi \Gamma_n(\theta)\frac{1}{r}\frac{\partial\psi(r,\theta)}{\partial\theta}\frac{\partial T(r,\theta)}{\partial r}\mathrm{d}\theta = \frac{1}{r}\sum_{j=1}^{\infty}\sum_{k=1}^{\infty} B_{njk}^*\overline{\psi_k}(r)\frac{\partial\overline{T_j}(r)}{\partial r} \tag{10e}$$

$$B_{njk}^* = \int_0^\pi \Gamma_n(\theta)\Gamma_j(\theta)\chi_k^{'}(\theta)\mathrm{d}\theta \tag{10f}$$

$$\int_0^{\pi} \Gamma_n(\theta)\frac{1}{r}\frac{\partial\psi(r,\theta)}{\partial r}\frac{\partial T(r,\theta)}{\partial\theta}\mathrm{d}\theta = \frac{1}{r}\sum_{j=1}^{\infty}\sum_{k=1}^{\infty} B_{njk}\overline{T_k}(r)\frac{\partial\overline{\psi_j}(r)}{\partial r} \tag{10g}$$

$$B_{njk} = \int_0^{\pi} \Gamma_n(\theta)\chi_j(\theta)\Gamma_k^{'}(\theta)\mathrm{d}\theta \tag{10h}$$

After the transformation, Eqs. (9) can be rewritten as

$$\frac{\partial^2\overline{\psi_i}(r)}{\partial r^2} + \frac{1}{r}\frac{\partial\overline{\psi_i}(r)}{\partial r} - \frac{\mu_i^2}{r^2}\overline{\psi_i}(r) = -Ra\left(\sum_{j=1}^{\infty} a_{ij}\frac{\partial\overline{T_j}(r)}{\partial r} - \frac{1}{r}\sum_{j=1}^{\infty} a_{ij}^{*}\overline{T_j}(r)\right) \tag{11a}$$

$$\frac{\partial^2\overline{T_n}(r)}{\partial r^2} + \frac{1}{r}\frac{\partial\overline{T_n}(r)}{\partial r} - \frac{\lambda_n^2}{r^2}\overline{T_n}(r) + \overline{f_n} = \frac{1}{r}\sum_{j=1}^{\infty}\sum_{k=1}^{\infty} B_{njk}^{*}\overline{\psi_k}(r)\frac{\partial\overline{T_j}(r)}{\partial r} - \frac{1}{r}\sum_{j=1}^{\infty}\sum_{k=1}^{\infty} B_{njk}\overline{T_k}(r)\frac{\partial\overline{\psi_j}(r)}{\partial r} \tag{11b}$$

$$\overline{\psi_i}(r_0) = 0,\ \ \overline{\psi_i}(1) = 0, \tag{11c}$$

$$\overline{T_n}(r_0) = 0,\ \ \overline{T_n}(1) = 0. \tag{11d}$$

In order to solve the problem presented by Eqs. (11) with finite differences, a finite-difference network is constructed over the region, then the differential equations are discretized by using the second-order accurate central-difference formula, according to Özisik (1994), for the second and the first derivatives of the transformed temperature and stream-function.

$$\frac{\overline{\psi}_{i_r+1} - 2\overline{\psi}_{i_r} + \overline{\psi}_{i_r-1}}{\Delta r^2} + \frac{1}{r_0 + i_r\Delta r}\frac{\overline{\psi}_{i_r+1} - \overline{\psi}_{i_r-1}}{2\Delta r} - \frac{1}{(r_0 + i_r\Delta r)^2}\mu_i^2\overline{\psi}_{i_r} = \\ - Ra\left(\sum_{j=1}^{\infty} a_{ij}\frac{\overline{T}_{i_r+1} - \overline{T}_{i_r-1}}{2\Delta r} - \frac{1}{r_0 + i_r\Delta r}\sum_{j=1}^{\infty} a_{ij}^{*}\overline{T}_{i_r}\right) \tag{12a}$$

$$\frac{\overline{T}_{i_r+1} - 2\overline{T}_{i_r} + \overline{T}_{i_r-1}}{\Delta r^2} + \frac{1}{r_0 + i_r\Delta r}\frac{\overline{T}_{i_r+1} - \overline{T}_{i_r-1}}{2\Delta r} - \frac{1}{(r_0 + i_r\Delta r)^2}\lambda_n^2\overline{T}_{i_r} = \\ \left(\frac{1}{r_0 + i_r\Delta r}\right)\sum_{j=1}^{\infty}\sum_{k=1}^{\infty}\left(B_{njk}^{*}\overline{\psi}_{i_r}\frac{\overline{T}_{i_r+1} - \overline{T}_{i_r-1}}{2\Delta r} - B_{njk}\overline{T}_{i_r}\frac{\overline{\psi}_{i_r+1} - \overline{\psi}_{i_r-1}}{2\Delta r}\right) - \overline{f_n} \tag{12b}$$

with boundary conditions

$$\overline{\psi}_i(0) = 0, \quad \overline{\psi}_i(irmax) = 0 \ \ 1 \leqslant i \leqslant max \tag{12c}$$

$$\overline{T}_n(0) = 0, \quad \overline{T}_n(irmax) = 0 \ \ 1 \leqslant n \leqslant max \tag{12d}$$

The calculations were performed using the Mathematica software, and the inversion formulas were applied to obtain the final results for the originals temperature and stream-function.

3. RESULTS AND DISCUSSION

The results were obtained considering different values of the governing parameters, such as the Rayleigh number (Ra = 10, 50, 100, 500, 1000, 2000, 5000), the inner radius(r_0= 0.25 and 0.5) and the angle (θ=0, $\frac{\pi}{4}$, $\frac{\pi}{3}$, $\frac{\pi}{2}$, π).

The convergence for the temperature and the stream function are presented in Tab. 1 and 2, for $Ra = 100$ and r_0=0.5, where the truncation order for the expansions max, varies from 10 to 40. The values of temperature and stream function are presented in different locations of the analysed geometry, where r is varying from $r_0 = 0.5$ to 1 and θ is varying from 0 to π. It can be seen in Tab. 1 that the temperature converged to four digits when the truncation order is equal to 20, and Tab. 2 reveals that the convergence for four digits occurs when the truncation order is also equal to 20.

Table 1: Convergence of temperature distribution

θ	max	r = 0.5	r = 0.6	r = 0.7	r = 0.75	r = 0.8	r = 0.9	r = 1.0
0	10	0.00000	0.02158	0.03075	0.03128	0.02936	0.01879	0.00000
	20	0.00000	0.02159	0.03076	0.03129	0.02937	0.01879	0.00000
	22	0.00000	0.02159	0.03076	0.03129	0.02937	0.01879	0.00000
	25	0.00000	0.02159	0.03076	0.03129	0.02937	0.01879	0.00000
	30	0.00000	0.02159	0.03076	0.03129	0.02937	0.01879	0.00000
	40	0.00000	0.02159	0.03076	0.03129	0.02937	0.01879	0.00000
$\frac{\pi}{4}$	10	0.00000	0.02164	0.03082	0.03135	0.02944	0.01884	0.00000
	20	0.00000	0.02165	0.03083	0.03136	0.02944	0.01885	0.00000
	22	0.00000	0.02166	0.03083	0.03136	0.02945	0.01885	0.00000
	25	0.00000	0.02166	0.03083	0.03136	0.02945	0.01885	0.00000
	30	0.00000	0.02166	0.03083	0.03136	0.02945	0.01885	0.00000
	40	0.00000	0.02166	0.03083	0.03137	0.02945	0.01885	0.00000
$\frac{\pi}{3}$	10	0.00000	0.02169	0.03087	0.03141	0.02949	0.01889	0.00000
	20	0.00000	0.02170	0.03088	0.03142	0.02950	0.01889	0.00000
	22	0.00000	0.02170	0.03088	0.03142	0.02950	0.01889	0.00000
	25	0.00000	0.02170	0.03088	0.03142	0.02950	0.01889	0.00000
	30	0.00000	0.02170	0.03088	0.03142	0.02950	0.01889	0.00000
	40	0.00000	0.02170	0.03088	0.03142	0.02950	0.01889	0.00000
$\frac{\pi}{2}$	10	0.00000	0.02180	0.03100	0.03154	0.02962	0.01899	0.00000
	20	0.00000	0.02181	0.03101	0.03155	0.02963	0.01899	0.00000
	22	0.00000	0.02181	0.03101	0.03155	0.02963	0.01899	0.00000
	25	0.00000	0.02181	0.03101	0.03155	0.02963	0.01899	0.00000
	30	0.00000	0.02181	0.03101	0.03155	0.02963	0.01899	0.00000
	40	0.00000	0.02181	0.03101	0.03155	0.02963	0.01900	0.00000
π	10	0.00000	0.02204	0.03127	0.03181	0.02990	0.01921	0.00000
	20	0.00000	0.02204	0.03128	0.03182	0.02991	0.01921	0.00000
	22	0.00000	0.02204	0.03128	0.03182	0.02991	0.01921	0.00000
	25	0.00000	0.02205	0.03128	0.03182	0.02991	0.01921	0.00000
	30	0.00000	0.02205	0.03128	0.03182	0.02991	0.01921	0.00000
	40	0.00000	0.02205	0.03128	0.03182	0.02991	0.01921	0.00000

Table 2: Convergence of stream function distribution

θ	max	r = 0.5	r = 0.6	r = 0.7	r = 0.75	r = 0.8	r = 0.9	r = 1.0
0	10	0.0000	0.0000	0.0000	0.0000	0.0000	0.0000	0.0000
	20	0.0000	0.0000	0.0000	0.0000	0.0000	0.0000	0.0000
	22	0.0000	0.0000	0.0000	0.0000	0.0000	0.0000	0.0000
	25	0.0000	0.0000	0.0000	0.0000	0.0000	0.0000	0.0000
	30	0.0000	0.0000	0.0000	0.0000	0.0000	0.0000	0.0000
	40	0.0000	0.0000	0.0000	0.0000	0.0000	0.0000	0.0000
$\frac{\pi}{4}$	10	0.0000	0.0567	0.0068	-0.0293	-0.0609	-0.0807	0.0000
	20	0.0000	0.0559	0.0058	-0.0303	-0.0618	-0.0812	0.0000
	22	0.0000	0.0559	0.0058	-0.0303	-0.0618	-0.0812	0.0000
	25	0.0000	0.0559	0.0057	-0.0304	-0.0619	-0.0813	0.0000
	30	0.0000	0.0558	0.0056	-0.0304	-0.0619	-0.0813	0.0000
	40	0.0000	0.0558	0.0056	-0.0305	-0.0620	-0.0814	0.0000
$\frac{\pi}{3}$	10	0.0000	0.0694	0.0082	-0.0361	-0.0748	-0.0990	0.0000
	20	0.0000	0.0685	0.0070	-0.0373	-0.0759	-0.0997	0.0000
	22	0.0000	0.0685	0.0069	-0.0373	-0.0759	-0.0997	0.0000
	25	0.0000	0.0684	0.0069	-0.0374	-0.0760	-0.0998	0.0000
	30	0.0000	0.0683	0.0068	-0.0375	-0.0761	-0.0998	0.0000
	40	0.0000	0.0683	0.0067	-0.0375	-0.0761	-0.0999	0.0000
$\frac{\pi}{2}$	10	0.0000	0.0801	0.0090	-0.0422	-0.0870	-0.1150	0.0000
	20	0.0000	0.0791	0.0077	-0.0436	-0.0882	-0.1158	0.0000
	22	0.0000	0.0790	0.0076	-0.0436	-0.0883	-0.1159	0.0000
	25	0.0000	0.0790	0.0075	-0.0437	-0.0884	-0.1159	0.0000
	30	0.0000	0.0789	0.0074	-0.0438	-0.0885	-0.1159	0.0000
	40	0.0000	0.0788	0.0073	-0.0439	-0.0885	-0.1160	0.0000
π	10	0.0000	0.0000	0.0000	0.0000	0.0000	0.0000	0.0000
	20	0.0000	0.0000	0.0000	0.0000	0.0000	0.0000	0.0000
	22	0.0000	0.0000	0.0000	0.0000	0.0000	0.0000	0.0000
	25	0.0000	0.0000	0.0000	0.0000	0.0000	0.0000	0.0000
	30	0.0000	0.0000	0.0000	0.0000	0.0000	0.0000	0.0000
	40	0.0000	0.0000	0.0000	0.0000	0.0000	0.0000	0.0000

The simulation time increases considerably according the value of max, from 40 seconds when $max = 10$, to 10733 seconds when $max = 40$. For $max = 20$ the simulation time is around 350 seconds.

Figures 2 and 3 presents comparisons between the results obtained with the generalized integral transform technique (GITT) and the finite difference method (FDM), which was developed to validate the GITT solution. The temperature and stream function profiles along the centreline of the cavity were analyzed considering $r_0 = 0.25$, $max = 20$, $Ra = 50$, and 500. It is possible to observe that the results for both methods are precise and accurate.

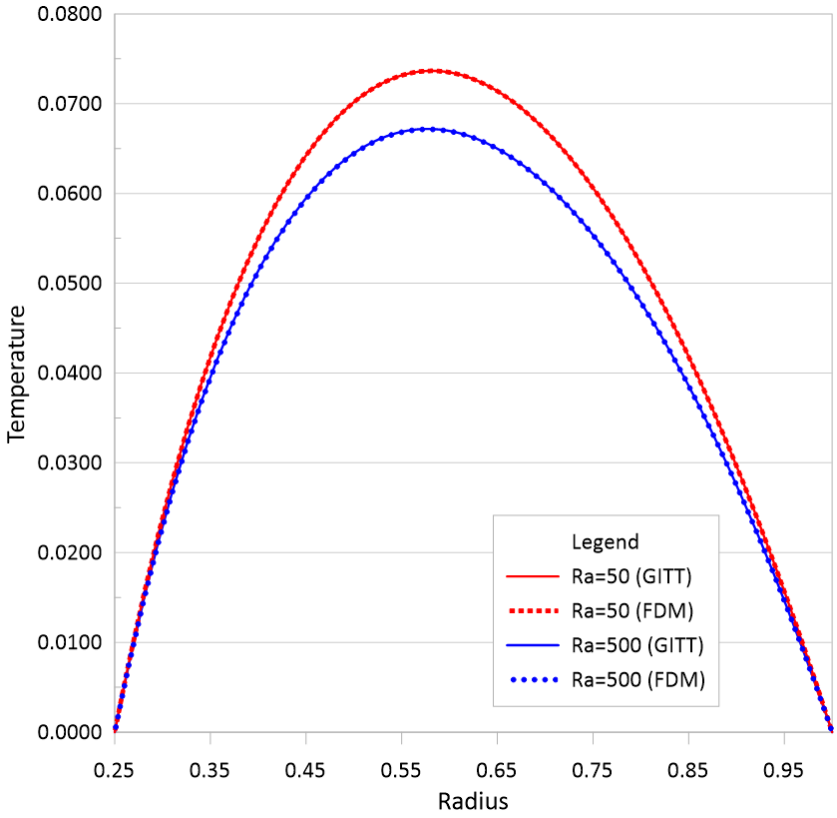

Figure 2: Comparison of GITT solution with FDM results: temperature profiles along the horizontal centreline ($\theta = \frac{\pi}{2}$)

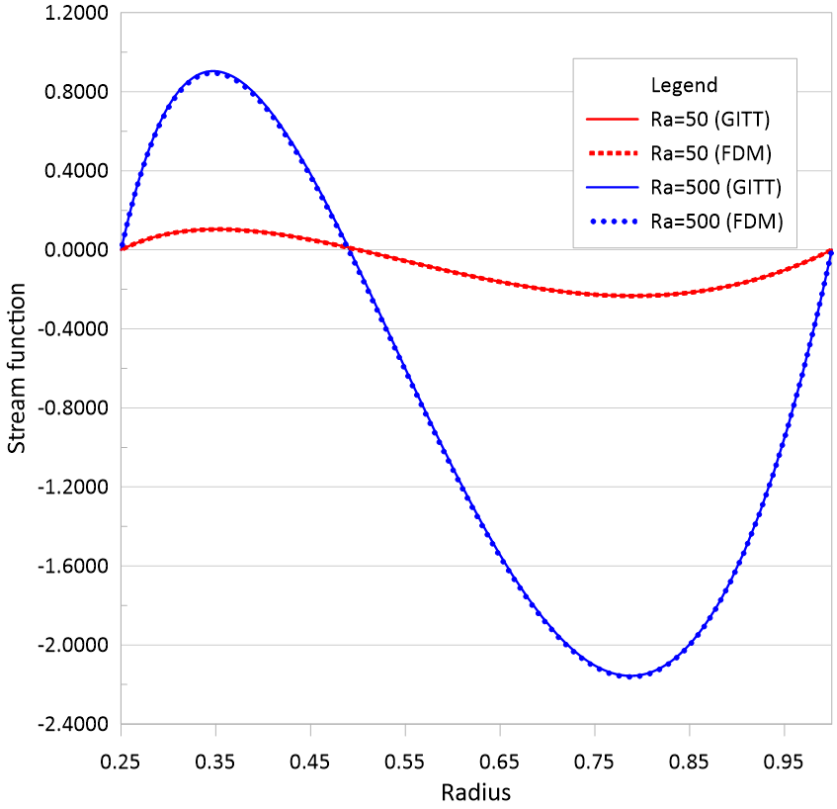

Figure 3: Comparison of GITT solution with FDM results: stream function profiles along the horizontal centreline ($\theta = \frac{\pi}{2}$)

Figure 4 show respectively the effect of natural convection on the radial distributions of the temperature, stream function, radial velocity and angular velocity at $\theta = \pi/2$ for Rayleigh number ranging 10 to 5000. The radius ranges from 0.5 to 1. As Ra is increased from 10 up to 5000, the temperature in the middle of the cavity decreases and the temperature profile gradually changes to a less sharp curve, with the maximum temperature in the core region and two boundary layers characterized by a strong temperature gradient. As Ra increases we observe the formation of more intense peaks of the stream function, and when it decreases the peak values are lower and the curves are smoother. The velocity vanishes at the point of separation of the vortexes. As Ra is increased, this separation point moves closer to the inner boundary and the downward flow becomes stronger than the upward flow.

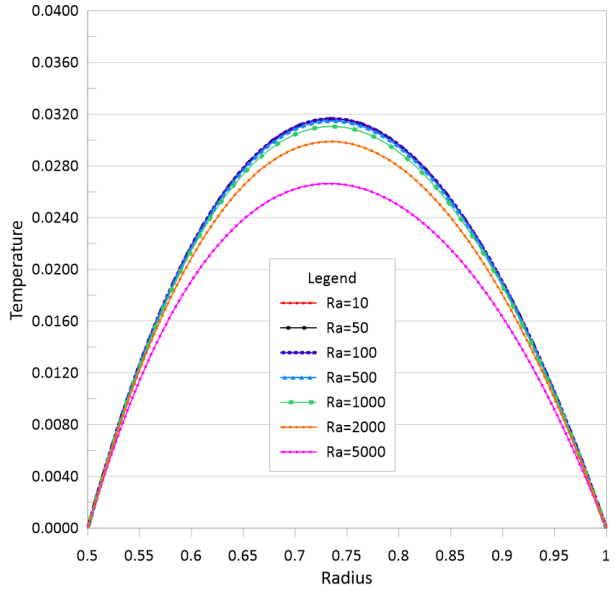

(a) Temperature

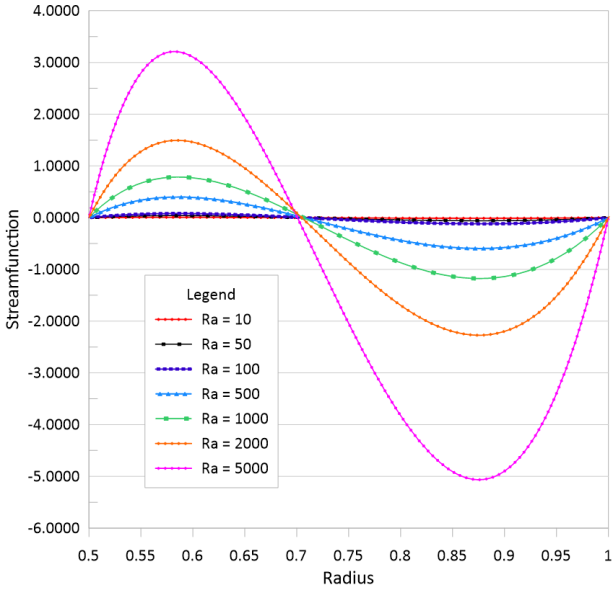

(b) Stream function

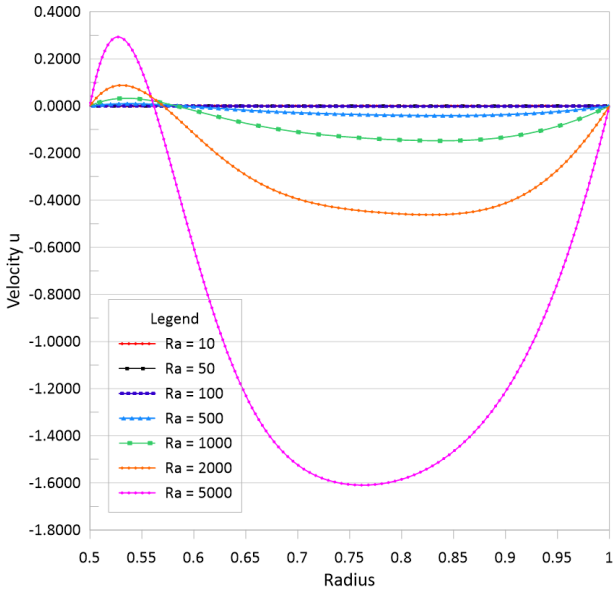

(c) Radial velocity (u)

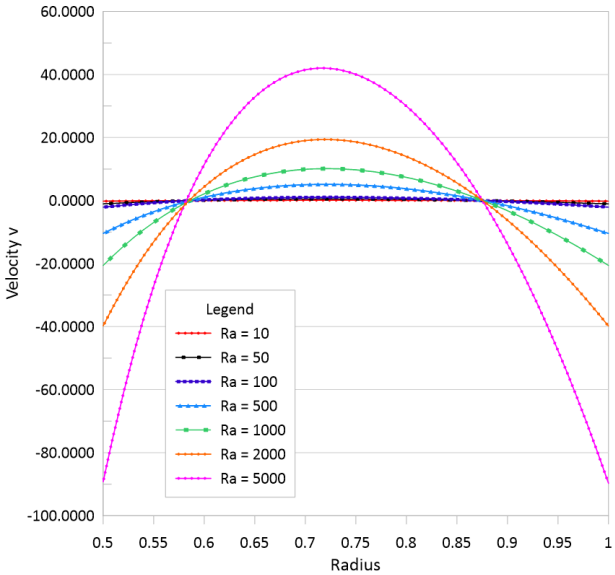

(d) Angular velocity (v)

Figure 4: Radial distributions at $\theta = \pi/2$ for Rayleigh number ranging from 10 to 5000.

4. CONCLUSIONS

Steady-state, laminar natural convection in a two-dimensional horizontal annulus filled with porous media with internal heat generation was investigated for a wide range of Rayliegh number $(10 \leq Ra \leq 5000)$. The convergence was verified for different truncation orders $(10 \leq max \leq 40)$, considering various locations within the cavity in order to verify the different mathematical and physical behaviour in the domain. The results obtained with the generalized integral transform technique were validate with the finite difference method, which indicates that the hybrid method is satisfactory and can solve the problem. It was noticed that in the horizontal direction, as the Rayleigh number increases, the maximum temperature in the temperature profiles decreases and the peaks of stream function are intensified, and when Ra decreases the stream function peak values are lower and the curves are smoother.

5. ACKNOWLEDGEMENTS

The authors are grateful to CNPq and FAPERJ for the financial support.

6. REFERENCES

Baohua, C. and Cotta, R.M., 1993. "Integral transform analysis of natural convection in porous enclosures". *International Journal for Numerical Methods in Fluids*, Vol. 17, No. 9, pp. 787–801.

Holzbecher, M. and Steiff, A., 1995. "Laminar and turbulent free convection in vertical cylinders with internal heat generation". *International Journal of Heat and Mass Transfer*, Vol. 38, No. 15, pp. 2893 – 2903.

Joshi, M.V., Gaitonde, U.N. and Mitra, S.K., 2006. "Analytical study of natural convection in a cavity with volumetric heat generation". *Journal of Heat Transfer*, Vol. 128, No. 2, pp. 176–182.

Lee, J. and Goldstein, R., 1988. "An experimental study on natural convection heat transfer in an inclined square enclosure containing internal energy sources". *Journal of Heat Transfer*, Vol. 110, No. 2, pp. 345–349.

Martin, B.W., 1967. "Free convection in a vertical cylinder with internal heat generation". *Proceedings of the Royal Society of London Series A-Mathematical and Physical Sciences*, Vol. 301, No. 4, pp. 327–341.

Shekar, B.C., Vasseur, P., Robillard, L. and Nguyen, T., 1984. "Natural convection in a heat generating fluid bounded by two horizontal concentric cylinders". *Canadian Journal of Chemical Engineering*, Vol. 62, No. 4, p. 482–489. doi:https://doi.org/10.1115/1.2910914.

Vasseur, P., Hung Nguyen, T., Robillard, L. and Tong Thi, V.K., 1984. "Natural convection between horizontal concentric cylinders filled with a porous layer with internal heat generation". *International Journal of Heat Mass Transfer*, Vol. 27, No. 3, pp. 337–349.

Yuan, X., Tavakkoli, F. and Vafai, K., 2015. "Analysis of natural convection in horizontal concentric annuli of varying inner shape". *Numerical Heat Transfer Part A: Applications*, Vol. 68, No. 11, pp. 1155–1174. doi: 10.1080/10407782.2015.1032016.

Özisik, M.N., 1994. *Finite Difference Methods in Heat Transfer*. CRC Press, 1st edition.

7. RESPONSIBILITY NOTICE

The authors are solely responsible for the printed material included in this paper.